Existence of a proton halo in ^{23}Al and its significance

X. Z. Cai,[1] H. Y. Zhang,[1] W. Q. Shen,[1,2,5] Z. Z. Ren,[4] J. Feng,[1] D. Q. Fang,[1] Z. Y. Zhu,[1] W. Z. Jiang,[1] Y. G. Ma,[1,2] C. Zhong,[1] W. L. Zhan,[3] Z. Y. Guo,[3] G. Q. Xiao,[3] J. S. Wang,[3] Y. T. Zhu,[3] J. C. Wang,[3] J. X. Li,[3] M. Wang,[3] J. F. Wang,[3] Z. J. Ning,[3] Q. J. Wang,[3] and Z. Q. Chen[3]

[1]*Shanghai Institute of Nuclear Research, Chinese Academy of Sciences, Shanghai 201800, China*

[2]*CCAST (World Laboratory), P.O. Box 8730, Beijing 100080, China*

[3]*Institute of Modern Physics, Chinese Academy of Sciences, Lanzhou 730000, China*

[4]*Physics Department of Nanjing University, Nanjing 210008, China*

[5]*Physics Department of Ningbo University, Ningbo 315211, China*

(Received 21 June 2001; published 16 January 2002)

Reaction cross section σ_R of proton-rich isotones ($N=10$) near ^{23}Al and Al isotopes ($^{23-28}$Al) on C target have been measured at intermediate energies around 30 MeV/nucleon. An abnormal increase of the experimental σ_R is observed for ^{23}Al and it suggests that there is an anomalously large matter rms radius in ^{23}Al. Together with the very weakly binding of the last proton ($S_p=0.125$ MeV), it indicates that there is a proton halo in ^{23}Al. This conclusion is also supported by the difference factor d which is deduced from the measured and theoretical σ_R in the Glauber or Boltzmann-Uehling-Uhlenbeck model and is used for the manifest of halo phenomena. The theoretical calculation based on the relativistic density dependent Hartree model shows that there is a proton halo when the last proton is in the $2s_{1/2}$ orbit in ^{23}Al. The significance of the proton halo in ^{23}Al is discussed.

DOI: 10.1103/PhysRevC.65.024610 PACS number(s): 25.60.Dz, 21.10.Ft, 27.30.+t

The experimental progress of radioactive ion beams has made it possible to study the phenomena of nuclei far from the β stability. Since the pioneering work by Tanihata *et al.* in 1985 [1], it is well known that there are neutron halos in light neutron-rich nuclei. The first experimental result on neutron halo is from the measurement of reaction cross section σ_R of Li isotopes where an abnormally large σ_R was observed for ^{11}Li [1] and it indicates there is neutron halo in ^{11}Li. Further experiments on σ_R confirm the neutron halo in ^{11}Li and also show the existence of neutron halo in other neutron-rich nuclei [1–11]. However, the experiments on the proton halo are relatively less as compared with those on neutron halo. Recently experimental evidence for proton halo or proton skin in very proton-rich nuclei has become available. Some experiments show that there is a pygme proton halo in a proton-rich nucleus ^{8}B [10–15]. Ozawa *et al.* [16] found that the radius of ^{17}Ne is larger than that of its mirror nucleus ^{17}N by measuring the interaction cross section of the $A=17$ isobars. It indicates that there is a proton halo in ^{17}Ne [16]. For its neighboring nuclei there may exist proton skins or halos [17–20], such as the existence of proton halo in the first excited state of ^{17}F. Some theoreticians, using the relativistic mean-field (RMF) model and a shell model, predicted that there are one-proton halos in ^{26,27,28}P and two-proton halos in ^{27,28,29}S [21–23]. The measurement of the momentum distribution confirms the existence of a proton halo in ^{26,27,28}P [24]. Based on an empirical formulas for matter root-mean-square (rms) radii of nuclei and RMF calculations, Wang and Shen *et al.* [25] predict one-proton halo in ^{23}Al. In this paper we report an experimental measurement of reaction cross section for proton-rich nuclei around ^{23}Al ($N=10$ isotones and $Z=13$ isotopes) and an abnormally large increase of σ_R for ^{23}Al is observed in the experiment. It is concluded that there is a proton halo in ^{23}Al based on the systematic analysis of experimental data.

The experiment was performed at the Heavy Ion Research Facility (HIRFL) of the Institute of Modern Physics (IMP) at Lanzhou. Secondary radioactive ion beams were produced by Radioactive Ion Beam Line (RIBLL) in HIRFL through the projectile fragmentation of a 69 MeV/nucleon ^{36}Ar primary beam. The carbon target of the thickness 109.7 mg/cm^2 was used. The isotopes were separated by means of magnetic rigidity ($B\rho$) and energy degrader (ΔE) as described in Ref. [9]. The selected isotopes were further identified by the time of fight (TOF) and energy loss (ΔE) in a transmission Si surface barrier detector before incidence on a reaction target. Behind the reaction target a telescope was installed, which consisted of five transmission Si surface barrier detectors and gave the energy losses (ΔE's) and total energy of the reaction products. The thicknesses of the six Si detectors were 150, 150, 150, 700, 700, and 2000 μm, respectively, and the energy resolutions were not greater than 1.8%. The details can be found in Ref. [9]

The reaction cross section σ_R is measured by the transmission-type experimental method, which relates the number of ions incident on the target ($N_{\rm inc}$) to the ions passing the target without interaction ($N_{\rm out}$) [1,10,9]

$$\sigma_R=\frac{A}{N_A t}\ln\left[\frac{N_{\rm inc}}{N_{\rm out}}\right], \quad (1)$$

where A is the mass number, of the target, N_A is Avogadro's number, and t is the thickness of the target in units of g/cm^2. The incident energies of secondary ion beams in the middle of the carbon target vary from 25 MeV/nucleon to 36 MeV/nucleon. The total energy-deposition spectra after the reaction target is used to extract the noninteraction particles passing the target, where the peak near total incident energy is defined as the noninteraction peak. Here inelastic scattering or any reaction not changeing proton and/or neutron number

TABLE I. Reaction cross section for $N=10$ isotones and $Z=13$ isotopes with ^{12}C target at intermediate energies.

	Projectile energy (MeV/nucleon)	σ_R(mb)
^{19}F	25.0	1620 ± 126
^{20}Ne	28.6	1668 ± 87
^{21}Na	31.0	1579 ± 100
^{22}Mg	33.4	1531 ± 125
^{23}Al	35.9	1892 ± 145
^{24}Al	32.8	1774 ± 94
^{25}Al	27.4	1629 ± 80
^{26}Al	24.7	1627 ± 108
^{27}Al	22.0	1733 ± 100
^{28}Al	19.0	1866 ± 121

in the incident nucleus are not included in the measured σ_R. The fragment with different charge Z could be separated and the isotope could not be identified by this detector system. But in this case, we just extract the number of ions passing the target without interaction and the fragment is not identified uniquely. The experimental data of σ_R for $N=10$ isotones and $Z=13$ isotopes are presented in Table I. It is seen that there is a sudden increase of σ_R for ^{23}Al. In the table the errors of σ_R refer to the statistical error plus the mean systematic error ($\pm4\%$) of extrapolating the reaction events of low-Q-value reactions into the middle of the nonreacted ion's peak. In order to see the variation of σ_R with the proton number, we draw the experimental data of $N=10$ isotones in Fig. 1(b), where the old data of Li isotopes from Tanihata *et al.* [1] are also plotted for comparison [Fig. 1(a)]. The σ_R

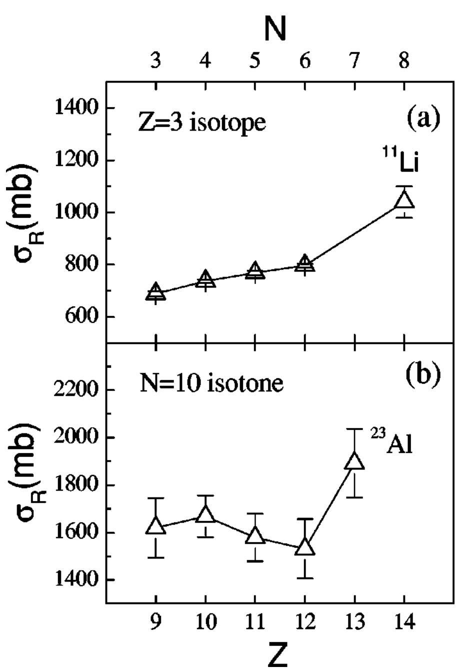

FIG. 1. The variation of σ_R with proton number Z for $N=10$ isotones where the old result of Li isotopes as a function of neutron number is also shown for comparison [1]. The dotted line shows the calculated σ_R'.

data at different energies are converted to σ_R on ^{12}C target at 30 MeV/nucleon using the parametrized formula [28]. σ_R can be calculated by $\sigma_R=\pi[R(p)+R(t)]^2$ where $R(p)$ is the projectile radius and $R(t)$ is the target radius which are calculated using $r_0A^{1/3}$ and r_0 is the radius parameter. This equation is always used to calculate the interaction cross sections at relativistic energies [1,3]. However, the σ_R at intermediate energies is larger than that at high energies and the parameter r_0 used at high energies is not suitable at intermediate energies. The ratio $=\sigma_R(\text{exp;medium})/\sigma_R(\text{cal;high})$ for stable nuclei is calculated, where $\sigma_R(\text{exp;medium})$ is the experimental σ_R at intermediate energies and $\sigma_R(\text{cal;high})$ is the σ_R at relativistic energies calculated using the above equation. It is found that the ratio is constant within the error bar of the experimental σ_R's. To see the mass dependence of σ_R, $\sigma_R'=\sigma_R\times$ratio is plotted in the figure by a dotted line. From Fig. 1 the σ_R data can be roughly reproduced by σ_R' except for ^{23}Al. It is seen more clearly that there is an anomalously large increase of σ_R for ^{23}Al. This behavior of σ_R is very similar to that of Li isotopes. Tanihata *et al.* [1] concluded that there is an abnormally large radius of ^{11}Li and the neutron halo appears in this nucleus. In view of the very similar behavior for the Li isotope [Fig. 1(a)] and the $N=10$ isotone [Fig. 1(b)], we conclude that the abnormally large cross section in ^{23}Al may indicate an appearance of proton halo in this nucleus. If we review the experimental proton separation energy of ^{23}Al, we notice its proton separation energy is very small $S_p=0.125$ MeV [26]. This demonstrates the last proton is very weakly bound in this nucleus. The proton separation energy in its neighboring nucleus ^{22}Mg is as high as $S_p=5.497$ MeV [26]. So ^{22}Mg is possibly a good inert core in ^{23}Al. This supports that there can be a proton halo in ^{23}Al.

In order to quantitatively analyze the possibility of nucleon halo in exotic light nuclei from the measured σ_R, Ozawa *et al.* [27] propose a difference factor d to manifest the appearance of halo. If d in a nucleus is evidently larger than that in its neighboring nuclei, there will appear nucleon halo in this nucleus. Ozawa *et al.* successfully apply this difference factor d to explain the appearance of an anomalous nucleon distributions such as neutron halo and neutron skin for ^{15}C in C isotopes and others. Here we use the difference factor d to see whether there is a proton halo in ^{23}Al. The difference factor d is defined [27] as

$$d=\frac{\sigma_R(\text{exp})-\sigma_R(\text{cal})}{\sigma_R(\text{cal})}, \tag{2}$$

where $\sigma_R(\text{exp})$ is the experimental data at intermediate energy and the theoretical value $\sigma_R(\text{cal})$ at intermediate energy is calculated with the width parameter obtained by fitting the experimental σ_R data at relativistic energy or the calculated σ_R data by using the parametrized formula [28] for those nuclei with no experimental data at relativistic energy.

Ozawa *et al.* calculated the difference factor d of C isotopes by the Glauber model [29]. Here we calculate the difference factor d by both the Glauber model and the Boltzmann-Uehling-Uhlenbeck (BUU) model [30–33]. Ac-

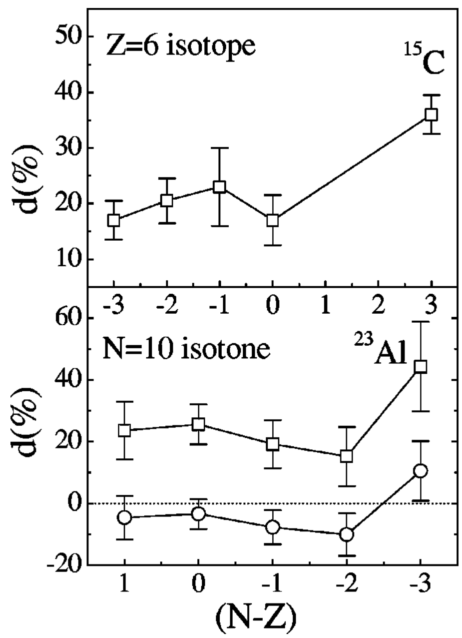

FIG. 2. The $(N-Z)$ dependence of d for $N=10$ isotones where the old result of C isotopes is drawn also for comparison [27]. The solid curve connecting the open square indicates the results of Glauber calculations. The solid curve connecting the open circles indicates the results of BUU calculations.

cording to our experiences [32,33], the BUU model is better than the Glauber model for the description of σ_R at intermediate energy. The factor d of halo nuclei is also larger than that of an ordinary nucleus in the BUU model. Thus it is considered that the difference factor d is sensitive to the exotic structure such as halo or skin phenomena. For a consistent comparison, the experimental values are converted to the values at 30 MeV/nucleon by using the parametrized formula [28]. The variation of the difference factor d with the neutron (or proton) excess $(N-Z)$ is plotted in Fig. 2 for $N=10$ isotones [Fig. 2(b)], where the variation of d with $(N-Z)$ for C isotopes from Ozawa *et al.* [27] is also drawn for comparison [Fig. 2(a)]. From Fig. 2 it is seen again that d for ^{23}Al is deviated from the normal trend and is remarkably larger than its neighbor nuclei. Here the results from the two models BUU and Glauber give the same trend for $N=10$ isotones. Ozawa *et al.* conclude that there is a neutron halo in ^{15}C [Fig. 2(a)]. We can draw the similar conclusion that there is a proton halo in ^{23}Al. Very recently the GANIL experiment with another method confirms that there is a neutron halo in ^{15}C [34]. This demonstrates that the analysis method of the difference factor d is reliable for halo phenomena of exotic nuclei [27]. Therefore the conclusion of a proton halo in ^{23}Al should be reliable.

So as to further elucidate the existence of proton halo in ^{23}Al, we measured σ_R of the secondary Al beams ($^{23-28}$Al) under the same experimental condition as listed in Table I. The data are also plotted in Fig. 3. Usually σ_R increases smoothly with the mass number A for an isotope series because σ_R is proportion to the square of the matter rms radius of a nucleus. This is seen from Fig. 3 for nuclei ^{26,27,28}Al, where the cross sections increase with the increase of mass

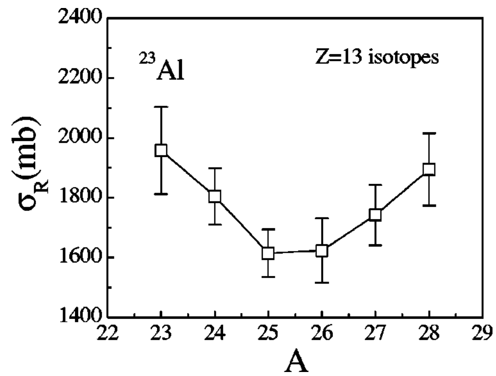

FIG. 3. The variation of the measured σ_R with the mass number A for Al isotopes.

number. When it approaches to the proton drip line (from ^{25}Al to ^{23}Al), σ_R increases with the decrease of the mass number. This contrary trend to the expected one is an indication of the appearance of proton skins or halos in these proton-rich nuclei. The cross section of ^{24}Al increases for a reference nucleus ^{25}Al. This indicates there is possibly a proton skin in ^{24}Al. The proton separation energy of ^{24}Al is 1.871 MeV. This agrees with the assumption of proton skins. But for the nucleus ^{23}Al, the cross section enhanced strongly, compared with its neighboring nuclei. Especially this happens even if its mass number is the smallest in this isotope series. This evidences that there is a proton halo in ^{23}Al. Its proton separation energy is also small $S_p=0.125$ MeV. This is consistent with the picture of a proton halo.

After we analyze the experimental data around ^{23}Al and conclude there is a proton halo in it, we now investigate the possible cause for the appearance of proton halo. In the ground state of ^{23}Al, the last proton can occupy the level $1d_{5/2}$ or $2s_{1/2}$ in the spherical shell model. When the last proton occupies $1d_{5/2}$, a large centrifugal barrier will tend to suppress the formation of a halo. This effect might be important for the formation of a halo in proton-rich nuclei. It is same for neutron-rich nuclei that a halo neutron may favor an orbit $2s_{1/2}$ in a spherical shell model (such as in ^{11}Li, ^{14}Be, ^{15}C). If there exist deformations in nuclei, the situation can become complex because both prolate and oblate deformations can appear. The configuration of the ground state changes for different values of deformation parameters. In this case the theoretical description of a halo will be complicate (such as in ^{11}Be and ^{19}C). Here it is unclear which case the nucleus ^{23}Al will belong to. The experimental ground state spin and parity of this nucleus is not available now. For its neighboring nucleus ^{22}Mg, there is a strong quadrupole deformation $\beta_2=0.56$ [35]. This may suggest that the case of ^{23}Al is similar to that in ^{11}Be and ^{19}C. The core nuclei ^{10}Be and ^{18}C in both ^{11}Be and ^{19}C are strongly deformed according to experimental data and theoretical calculations. At present a complete description of the neutron halo for both ^{11}Be and ^{19}C is still pending. So a correct description of the proton halo in ^{23}Al may bring a new challenge to the present theoretical models. Here we use a simple relativistic density dependent Hartree (RDDH) model to investigate the proton halo in ^{23}Al [36]. We assume the last

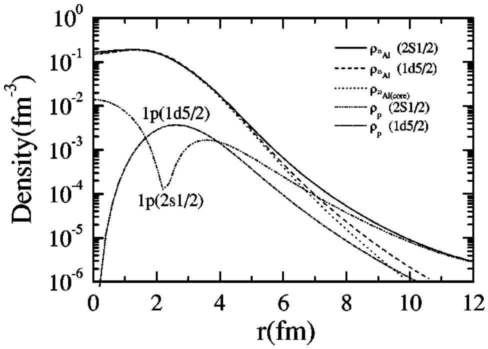

FIG. 4. Density distributions of ^{23}Al and ^{22}Mg. The solid and dashed curves are the matter density distributions of ^{23}Al where the last proton occupies the $2s_{1/2}$ or $1d_{5/2}$ orbits, respectively. The dotted-dotted-dashed and dotted-dashed curves are the density distributions of the last proton where the last proton occupies the $2s_{1/2}$ or $1d_{5/2}$ orbits, respectively. The dotted curve is the matter distribution of ^{22}Mg, the core of ^{23}Al.

proton occupies the spherical levels $1d_{5/2}$ or $2s_{1/2}$, then we obtain the matter density distributions of ^{23}Al, with the inert core ^{22}Mg, and the last proton which fills in $1d_{5/2}$ or $2s_{1/2}$. The results of density distributions are depicted in Fig. 4 where the proton separation energy is adjusted to the experimental value $S_p=0.125$ MeV and a spherical code is used. It is seen from Fig. 4 that an extended density distribution (i.e., a long tail) appears when the last proton occupies $2s_{1/2}$. The Δ rms, which equals to the difference between proton rms radius and neutron rms radius, of the last proton in $2s_{1/2}$ and in $1d_{5/2}$ is 0.42 and 0.28 fm, respectively. This corresponds to a proton halo in the $2s_{1/2}$ in ^{23}Al.

Due to the systematic underestimation of σ_R in the Glauber model at intermediate energies [27], σ_R is calculated by $\sigma_R=\sigma_R(\mathrm{Gl})\times\epsilon(E)$ in order to extract the experimental density distribution. $\epsilon(E)$ is an energy dependent factor, which is obtained by a linear fit to the ratio $\sigma_R(\exp)/\sigma_R(\mathrm{Gl})$ at energy around several tens MeV/nucleon [37]. We assume that the functional shape for proton density distribution in ^{23}Al is composed of HO-type core plus Yukawa-square tail at the outer region [7,37]. The width parameter of the HO-type core is fitted to σ_R of ^{22}Mg. The only parameter of the Yukawa-square tail distribution is obtained by fitting the experimental data of ^{23}Al. Then the rms radii of ^{23}Al are obtained from the experimental density distributions, which are extracted from experimental σ_R using the above modified Glauber model. The extracted Δ rms of ^{23}Al is 0.463 ± 0.150 fm, which is consistent with the result of RDDH calculation with the last proton occupying the $2s_{1/2}$ orbital. Therefore the proton halo will appear when the last proton is in $2s_{1/2}$. It should be mentioned that we have used a simple Glauber model and a BUU model to analyze the data. Recently an improvement on a simple Glauber model is made by Al-Khalili and Tostevin [38,39]. They introduced an appropriate cluster-Glauber theory to extract the matter radii of halo nuclei ^{11}Li, ^{11}Be, and ^{8}B, by considering the intrinsic few-body structure of these exotic projectiles and the adiabatic nature of the projectile-target interaction [38,39]. They showed that the significantly larger matter radii of halo nuclei than previously reported are needed in order to reproduce the experimental data. If their method is used for proton-rich nuclei in this paper, it is expected that the proton halo in ^{23}Al will be more evident than here reported. The conclusion that there is a proton halo in ^{23}Al will not change even if another analysis method is used.

The proton halo nucleus ^{23}Al is between halo nuclei ^{17}Ne and ^{26,27,28}P. It may play an important role for the study of proton halos in $2s$-$1d$ shell nuclei. It bridges the gap between ^{17}Ne and ^{26,27,28}P. This is very useful to elucidate the mechanism of the appearance of proton halo in $2s$-$1d$ shell. Very recently Ozawa *et al.* proposed that $N=16$ is a new magic number for some neutron-rich nuclei with the isospin $T_3 \geqslant 3$ [40]. It is unknown whether it is true for proton-rich nuclei. The proton halo appears for proton-rich nuclei with proton number $Z \leqslant 16$. The isospin of these nuclei is approximately $T_3 \geqslant \frac{3}{2}$. These may indicate that $Z=16$ could be a new magic number for these proton-rich nuclei. It is also known that there is a level inversion between $1d_{5/2}$ and $2s_{1/2}$ for $N=9$ neutron-rich isotones [41]. It is interesting to study if this inversion occurs for $N=10$ proton-rich isotones or $Z=13$ proton-rich isotopes. In the future it is also very interesting to measure the spin and parity of ^{23}Al to elucidate its ground state properties. The measurement of its quadrupole moments and magnetic moments will shed the light on its ground state deformation. No matter what, the error bars of the present experiment are large. Thus more measurements of σ_R at high or intermediate energies by more reliable and accurate method are necessary.

In summary, reaction cross sections σ_R of $N=10$ isotones (^{19}F–^{23}Al) and $Z=13$ isotopes (^{23}Al–^{28}Al) were measured at intermediate energies. An remarkable enhancement of σ_R for ^{23}Al was observed as compared with its neighboring nuclei. This result, together with the very small proton separation energy ($S_p=0.125$ MeV), strongly suggests the existence of proton halo in ^{23}Al. σ_R at intermediate energy was calculated with Glauber and BUU model by fitting the experimental one at relativistic energy. The different factor d (another quantity for the signature of halo phenomena) was deduced from the experimental and calculated data at intermediate energy. The difference factor d of ^{23}Al shows an abnormal increase compared to its neighbors, which also supports the existence of a proton halo in ^{23}Al. Further measurement of σ_R for Al isotopes was carried out and it confirms the abnormally large cross section for ^{23}Al. This shows again that there is a proton halo in ^{23}Al. The calculation of ^{23}Al with the relativistic density dependent Hartree model manifests the existence of proton halo in ^{23}Al when the last proton occupies the $2s_{1/2}$ level. The appearance of proton halo in ^{23}Al bridges the gap of halo phenomena between ^{17}Ne and ^{26,27}P. This is very important for elucidating the mechanism of the appearance of halo in $2s$-$1d$ shell. Further experiments and calculations will be necessary for a detailed study of the halo structure in ^{23}Al.

This work was supported by the Major State Basic Research Development Program in China under Contract No. G200077400 and by the National Natural Science Foundation of China.

[1] I. Tanihata, H. Hamagaki, O. Hashimoto, Y. Shida, N. Yoshikawa, K. Sugimoto, O. Yamakawa, T. Kobayashi, and N. Takahashi, Phys. Rev. Lett. **55**, 2676 (1985).
[2] I. Tanihata *et al.*, Phys. Lett. **160B**, 380 (1985).
[3] I. Tanihata *et al.*, Phys. Lett. B **287**, 307 (1992).
[4] P. G. Hansen and B. Jonson, Europhys. Lett. **4**, 409 (1989).
[5] W. Mittig *et al.*, Phys. Rev. Lett. **59**, 1889 (1987).
[6] M. G. Saint-Laurent *et al.*, Z. Phys. A **322**, 457 (1989).
[7] M. Fukuda *et al.*, Phys. Lett. B **268**, 339 (1991).
[8] T. Suzuki *et al.*, Phys. Rev. Lett. **75**, 3241 (1995).
[9] D. Q. Fang *et al.*, Phys. Rev. C **61**, 064311 (2000).
[10] R. E. Warner *et al.*, Phys. Rev. C **52**, R1166 (1995).
[11] B. Blank *et al.*, Nucl. Phys. **A624**, 242 (1997).
[12] M. M. Obuti, T. Kobayashi, D. Hirata, Y. Ogawa, K. Sugimoto, I. Tanihata, D. Olson, W. Christie, and H. Wieman, Nucl. Phys. **A609**, 74 (1996).
[13] C. Borcea *et al.*, Nucl. Phys. **A616**, 231 (1997).
[14] T. Minamisono *et al.*, Phys. Rev. Lett. **69**, 2058 (1992).
[15] W. Schwab *et al.*, Z. Phys. A **350**, 283 (1995).
[16] A. Ozawa *et al.*, Phys. Lett. B **334**, 18 (1994).
[17] L. Chulkov, E. Roeckl, and G. Kraus, Z. Phys. A **353**, 351 (1996).
[18] L. Chulkov *et al.*, Nucl. Phys. **A603**, 219 (1996).
[19] K. E. Rehm *et al.*, Phys. Rev. Lett. **81**, 3341 (1998).
[20] R. Morlock, R. Kunz, A. Mayer, M. Jaeger, A. Muller, J. W. Hammer, P. Mohr, H. Oberhummer, G. Staudt, and V. Kolle, Phys. Rev. Lett. **79**, 3837 (1997).
[21] Z. Z. Ren, B. Q. Chen, Z. Y. Ma, and G. O. Xu, Phys. Rev. C **53**, R572 (1996).
[22] B. A. Brown and P. G. Hansen, Phys. Lett. B **381**, 391 (1996).
[23] B. Q. Chen, Z. Y. Ma, F. Grummer, and S. Krewald, J. Phys. G **24**, 97 (1998).
[24] A. Navin *et al.*, Phys. Rev. Lett. **81**, 5089 (1998).
[25] J. S. Wang, W. Q. Shen, J. Feng, and W. Ye, Mem. Fac. Eng., Osaka City Univ. **19**, 23 (1997).
[26] A. H. Wapstra and G. Audi, Nucl. Phys. **A432**, 1 (1985).
[27] A. Ozawa, I. Tanihata, T. Kobayashi, Y. Sugahara, O. Yamakawa, K. Omata, K. Sugimoto, D. Olson, W. Christie, and H. Wieman, Nucl. Phys. **A608**, 63 (1996).
[28] W. Q. Shen, B. Wang, J. Feng, W. L. Zhan, Y. T. Zhu, and E. P. Feng, Nucl. Phys. **A491**, 130 (1989).
[29] R. J. Glauber, *Lectures on Theoretical Physics* (Interscience, New York, 1959), Vol. I.
[30] G. F. Bertsch and S. D. Gupta, Phys. Rep. **160**, 189 (1988).
[31] B. A. Li, Z. Z. Ren, C. M. Ko, and S. J. Yennello, Phys. Rev. Lett. **76**, 4492 (1996).
[32] Y. G. Ma, W. Q. Shen, J. Feng, and Y. Q. Ma, Phys. Rev. C **48**, 850 (1993).
[33] X. Z. Cai, J. Feng, W. Q. Shen, Y. G. Ma, J. S. Wang, and W. Ye, Phys. Rev. C **58**, 572 (1998).
[34] E. Sauvan *et al.*, Phys. Lett. B **491**, 1 (2000).
[35] S. Raman, C. H. Malarkey, W. T. Milner, C. W. Nestor, Jr., and P. H. Stelson, At. Data Nucl. Data Tables **36**, 1 (1987).
[36] W. Z. Jiang, Z. Y Zhu, and Z. Z. Ren, Phys. Lett. B (to be published).
[37] M. Fukuda *et al.*, Nucl. Phys. **A656**, 209 (1999).
[38] J. S. Al-Khalili and J. A. Tostevin, Phys. Rev. Lett. **76**, 3903 (1996).
[39] J. S. Al-Khalili, J. A. Tostevin, and I. J. Thompson, Phys. Rev. C **54**, 1843 (1996).
[40] A. Ozawa, T. Kobayashi, T. Suzuki, K. Yoshida, and I. Tanihata, Phys. Rev. Lett. **84**, 5493 (2000).
[41] Z. Z. Ren, B. Q. Chen, Z. Y. Ma, and G. O. Xu, Z. Phys. A **357**, 137 (1997).